Carbohydrate Polymers 86 (2011) 1221–1229

Contents lists available at ScienceDirect

Carbohydrate Polymers

journal homepage: www.elsevier.com/locate/carbpol

Crystal transition from cellulose I to cellulose II in NaOH treated *Agave americana* L. fibre

A. El Oudiani*, Y. Chaabouni, S. Msahli, F. Sakli

Unité de Recherches Textiles, ISET, University of Monastir, Avenue Ali Soua, 5070 Ksar Hellal, Tunisia

ARTICLE INFO

Article history:
Received 3 April 2011
Received in revised form 7 June 2011
Accepted 7 June 2011
Available online 22 June 2011

Keywords:
Alkalization
Cellulose I
Cellulose II
Mercerization
X-ray diffraction
Crystal structures
Textile

ABSTRACT

This study investigates the cellulose polymorphic transformation of *Agave americana* L. fibre during alkali processing at different NaOH concentrations. X-ray diffraction was used. The polymorphic transition from cellulose I to cellulose II begun at NaOH concentrations at the order of 5–10% and the complete transformation was achieved for the alkali concentration of 15%.

The crystallinity index of agave fibre increased for alkali treatments not exceeding 2% (w/v), whereas higher NaOH concentrations (>2%) induce a considerable decrease of the crystallinity index. The unit cell parameters of *A. americana* L. fibre vary with the NaOH concentration which results from the formation of different alkali celluloses during the mercerisation process.

As far as mechanical properties are concerned, treatments with low alkali concentrations produce fibres that are stronger than the untreated fibres, whereas treatments with high concentrations (>2% w/v) result in weaker fibres.

1. Introduction

Cellulose is a linear homopolymer of (1→4)-linked β-D-glucopyranose units (Glc) aggregated to form a highly ordered structure due to its chemical constitution and spatial conformation (Klemm et al., 1998). Three hydroxyl groups in each Glc are able to interact with one another forming intra and intermolecular hydrogen bonds. The use of cellulose in some applications is limited because it is soluble in few solvents and does not melt without thermal degradation. Hydrogen bonds in cellulose substrates are modified by some physical and/or chemical transformations for various applications. Typically, treatment with aqueous NaOH solution of a specific concentration (≈10 wt%) causes the transformation of cellulose I into cellulose II within the crystalline domains (Dinand, Vignon, Chanzy, & Heux, 2002; Jähn, Schröder, Füting, Schenzel, & Diepenbrock, 2002; Zugenmaier, 2001). This procedure is used for mercerization and viscose rayon manufacture in the textile and fibre industries (Kroschwitz, 1990). However, the concentration of NaOH for the complete transformation depends on the type of cellulose being treated. Common methods for the characterization of crystalline cellulose structure are based on X-ray (Dinand et al., 2002; Gert et al., 2001; Gumuskaya, Usta, & Kirci, 2003; Nishiyama, Langan, & Chanzy, 2002; Nishiyama, Sugiyama, Chanzy, & Langan, 2003) or electron diffraction (Atalla & VanderHart, 1999; Sugiyama, Vuong, & Chanzy, 1991), FT Raman (Atalla & VanderHart, 1999; Cael, Gardner, Koenig, & Blackwell, 1975; Jähn et al., 2002; Proniewicz et al., 2001) density determinations, infrared (IR) absorption (Akerholm, Hinterstoisser, & Salmen, 2004; Colom & Carrillo, 2002; Gert et al., 2001; Gumuskaya et al., 2003; Ruan, Zhang, Mao, Zeng, & Li, 2004; Schwanninger, Rodrigues, Pereira, & Hinterstoisser, 2004) and nuclear magnetic resonance (NMR) (Atalla & VanderHart, 1999; Newman & Davidson, 2004). Amongst them, wide-angle X-ray diffraction gives the most direct results and quantitative information. The polymorphic transformation of cellulose I to cellulose II has been studied with X-ray diffraction in many cellulosic fibres (Beg & Pickering, 2004; Bledzki, Fink, & Specht, 2004; Gassan & Bledzki, 1999a,b; Mirjana, Biljana, & Petar, 2008; Mwaikambo & Ansell, 2003; Ouajai & Shanks, 2005; Prasad & Sain, 2003; Zhou, Yeung, Yuen, & Zhou, 2004). However, the mercerisation of agave fibre has not yet been investigated. The present work deals with the influence of NaOH concentration on the mercerization degree of cellulose present in *Agave americana* L. fibre and the transformation from cellulose I to cellulose II polymorphs. This study is based on the X-ray diffraction method.

2. Experimental

2.1. Sampling

A. americana L. is the vegetation of Amaryllidaceae cultivated in North Africa and originated from Central America. Since 1998, the

* Corresponding author. Tel.: +216 22 930 867; fax: +216 73 475 163.
E-mail address: asmaeloudiani@yahoo.fr (A.E. Oudiani).

0144-8617/$ – see front matter © 2011 Elsevier Ltd. All rights reserved.
doi:10.1016/j.carbpol.2011.06.037

basic fibres of this plant have been the subject of many researches and seemed to be interesting due to their mechanical and physical properties. These natural cellulosic fibres were characterized by a high hydrophilicity, a low density, a high tenacity and a great extensibility in comparison with other textile fibres (Msahli, 2002).

The leaves of *A. americana* L. present a composite structure with an organic matrix and a reinforcement composed of cellulose micro-fibres, which show different kinds of chemical bonding such as covalent, hydrogen or Van Der Waals bonds. The organic matrix is composed of several components including hemicelluloses, pectic matter, lignin and gums; whereas the reinforcing fibres are mainly composed of cellulose.

To extract fibres from the organic matrix, different methods can be used. These methods have a great influence on the fine structure of the obtained fibres. Acceptable mechanical properties have been obtained by the extraction of fibres in distilled water which is used here. In this method, leaves are submitted to a hydrolysis treatment in distilled water. Subsequently, fibres are separated from the matrix by calendering the leaf and then washed. A temperature of 120 °C and duration of 90 min appear to be the best conditions for the treatment as demonstrated in a previous study (Chaâbouni, 2005; El Oudiani, Chaâbouni, Msahli, & Sakli, 2009).

2.2. Alkali treatment

Dried fibres (5 g) were treated with various concentrations of NaOH solution (100 mL) and placed in an oven at 30 °C for 1 h in order to remove hemicelluloses and lignin associated with the fibres. The concentrations of NaOH solutions were 1, 2, 5, 10, 15, 20 and 30% (w/v) (by weight). The alkaline treated fibres were subsequently washed with running tap water followed by distilled water until no alkali was present in the wash water.

2.3. X-ray diffraction

Bundles of technical fibres were aligned manually and lacerated with a scalpel. Short segments of fibres were then obtained and placed into a sliding disk mill. The mill comprised a means of randomly mixing and distributing the small fibres lengths in various orientations at conditions of surface pressure far below those that would induce crystallite fracture. The sample mass was then placed into a standard holder within the stage of the diffractometer. The spectra were determined using a PANalytical X'Pert Pro MPD-spectrometer set at 45 kV and 40 mA. Samples were scanned from $2\theta = 5^\circ$ to $2\theta = 40^\circ$ with increments of 0.02° using the CuKα radiation ($\lambda = 1.54$ Å).

For the air scatter trace, the fibres were removed from the sample holder, the empty holder was reinserted and an X-ray trace was obtained under conditions similar to those for the fibre traces. Corrections for the array of intensities of *A. americana* L. fibres were made for air scatter and polarization (Berlant & Khalifa, 1991; Sotton, Arniaud, & Rabourdin, 1978) using the following formulas:

- Correction for the air scatter:

$$(I_1)_{2\theta} = (I)_{2\theta} - (I_{air})_{2\theta} \exp^{-\mu t/\cos\ \theta} \quad (1)$$

$(I)_{2\theta}$ = intensity of the fibres obtained by the spectrometer, $(I_{air})_{2\theta}$ = intensity obtained for the air scatter and μt = optical density of the prepared samples ($\mu t = 1.2$)

- Correction for the polarization effect:

$$(I_2)_{2\theta} = \frac{(I_1)_{2\theta}}{0.5(1+\cos^2\ 2\theta)} \quad (2)$$

The corrected array of intensities was replotted against the Bragg angles, and the background was removed for all the curves.

2.3.1. Spectral analysis

In order to obtain maximum use of the X-ray diffraction data, each peak profile was fit to the Pearson VII function (Kreze & Malej, 2003) of the form:

$$I(x) = \frac{A}{\left[1 + ((x - X_c)/w)^2 (2^{1/\mu} - 1)\right]^{\mu}} \quad (3)$$

where $I(x)$: intensity, x: 2θ, A: profile amplitude, w: profile width, X_c: profile center, μ: profile shape factor.

In this study, estimated values of X_c, A, w and μ for each peak profile, together with the corrected intensity data points and the Bragg angles (2θ) were used as input values in a software resolution program (Origin 06). The best minimization between observed and calculated intensities occurs when the estimated parameters are well chosen.

For each diffractogram, cellulose I and cellulose II components were resolved into four and three reflections, respectively. From the sum of peak area of the same crystal system ($\sum A_{CI}$ for cellulose I and $\sum A_{CII}$ for cellulose II), CI and CII percentages were calculated using Eqs. (4) and (5):

$$CI\,(\%) = \frac{\sum A_{CI}}{\sum (A_{CI} + A_{CII})} \times 100 \quad (4)$$

$$CII\ (\%) = \frac{\sum A_{CII}}{\sum (A_{CI} + A_{CII})} \times 100 \quad (5)$$

The percentage of each reflection peak (CI and CII peaks) is calculated by dividing the area of the peak into the total area using Eq. (6):

$$Peak\,(\%) = \frac{A_{peak}}{\sum A_{CI} + A_{CII}} \quad (6)$$

2.3.2. Crystallinity index

The crystallinity index (I_c) was calculated using the following formula (Tserki et al., 2005):

$$I_C = \left(\frac{I_{0\ 0\ 2} - I_{am}}{I_{0\ 0\ 2}}\right) \times 100 \quad (7)$$

where I_{002} is the maximum intensity of diffraction of the (002) lattice peak at a 2θ angle of between 22° and 23°, and I_{am} is the intensity of diffraction of the amorphous material, which is taken at a 2θ angle between 18° and 19° where the intensity is at a minimum (Roncero et al., 2005).

2.3.3. Lattice spacing

The lattice spacing d_{hkl} was determined for each profile from the resolved position X_c and using the Bragg equation (Morton & Hearle, 1975):

$$n\lambda = 2d\ \sin\ \theta \quad (8)$$

where n is an integer, λ the wave length of the X-rays, θ the angle of diffraction ($2\theta = X_c$), and d the distance between the atomic layers (lattice spacing).

2.3.4. Unit cell dimensions and monoclinic angle

X-ray spectra of *A. americana* L. fibres provide fibre reflections associated with four different orders, only one of which yields an axial dimension by a single-step calculation.

The b-axial dimension is determined directly from:

$$b = k\, d_{0\ k\ 0} \quad (9)$$

k: Miller indices (0 k 0)

The composite product of the *c*-axial dimension and the monoclinic angle is:

$$c \sin \beta = l\, d_{0\ 0\ l} \tag{10}$$

l: Miller indices (0 0 l)

The composite product of the *a*-axial dimension and the monoclinic angle is:

$$a \sin \beta = \frac{l}{\sqrt{0.5\left(d_{1\ 0\ 1}{}^{-2} + d_{1\ 0\ \bar{1}}{}^{-2}\right) - l^{-2} d_{0\ 0\ l}{}^{-2}}} \tag{11}$$

l: Miller indices (0 0 l)

The monoclinic angle can be found from:

$$\beta = \arccos\left[\frac{\left(d_{1\ 0\ \bar{1}}{}^{-2} - d_{1\ 0\ 1}{}^{-2}\right) l\, d_{0\ 0\ l}}{4\sqrt{\frac{1}{2}\left(d_{1\ 0\ \bar{1}}{}^{-2} + d_{1\ 0\ 1}{}^{-2}\right) - l^{-2} d_{0\ 0\ l}{}^{-2}}}\right] \tag{12}$$

Having found β, we determined *a* and *c* from the respective composite formulas (Forman & Jakes, 1993).

2.3.5. Crystallite size

The crystallite size normal to the *h k l* plane was calculated from the integral breadth *B* of the peak according to Scherrer's equation (Scherrer, 1918):

$$D_{\perp h\ k\ l} = \frac{K\lambda}{B \cos\ \theta} \tag{13}$$

where $D_{\perp h\,k\,l}$: crystallite dimension in the direction perpendicular to the crystallographic plane *h k l*, θ: Bragg angle, λ: wave length of the radiation, *k*: constant 0.9 (although this factor is sensitive to crystal type) (Davidson, Newman, & Ryan, 2004; Murdock, 1930).

2.4. Mechanical testing

Tensile tests were carried out using a Lloyd dynamometer with a constant strain rate. This latter was adjusted to a speed of 250 mm/mn for a 500 mm specimen length to respect the test duration of 20 ± 3 s specified in NFG 07002 French Standard. Tests were conducted under standard conditions: 20 °C ± 2 °C and 65% ± 2% RH. Because of the high variability found in the tests, we chose a sample size of 50 fibres for each test.

3. Results and discussion

3.1. Spectral analysis

X-ray diffraction traces with corrected intensities are shown in Fig. 1. The diffractogram of untreated fibres (0% (w/v) NaOH) shows a pattern quite similar with the four peaks characteristic of native cellulose (cellulose I). These peaks are approximately located at 2θ = 14°, 16°, 23° and 35°; which are the positions of the (1 0 1), (1 0 $\bar{1}$), (0 0 2) and (0 4 0) crystallographic plane reflections, respectively (Berlant & Khalifa, 1991; Davidson et al., 2004; Ouajai & Shanks, 2005; Sotton et al., 1978). Whereas for the NaOH concentration of 30% (w/v), the diffractogram peaks are typical of cellulose II polymorph following the mercerisation process of the fibre. These peaks are located at 2θ = 11°, 20°, 22° and 37° which correspond to the diffraction of (1 0 1), (1 0 $\bar{1}$), (0 0 2) and (0 4 0) crystallographic plane reflections, respectively (Beatriz, Assa, & Belgacemb, 2006; Chen, Nattakan, Ni, & Ton, 2008; Ouajai & Shanks, 2005; Raymond, Kvick, & Chanzy, 1995; Sang et al., 2005).

For low alkali concentrations (<10%), the two peaks present on the X-ray diffractograms at 2θ = 14° and 2θ = 16° correspond to the (1 0 1) and (1 0 $\bar{1}$) crystallographic planes, respectively. When the crystalline cellulose content is high, these two peaks are more pronounced, and when the fibre contains large amounts of amorphous material (such as lignin, hemicelluloses, pectins and amorphous cellulose), these two peaks are smeared and appear as one broad peak (Perel, 1990). It can be seen in Fig. 1 that the peaks at 14° and 16° are more defined for the alkali treated agave fibre (mainly for the NaOH concentration of 10%), therefore suggesting that the alkali treatment removed some of the amorphous materials from the fibre.

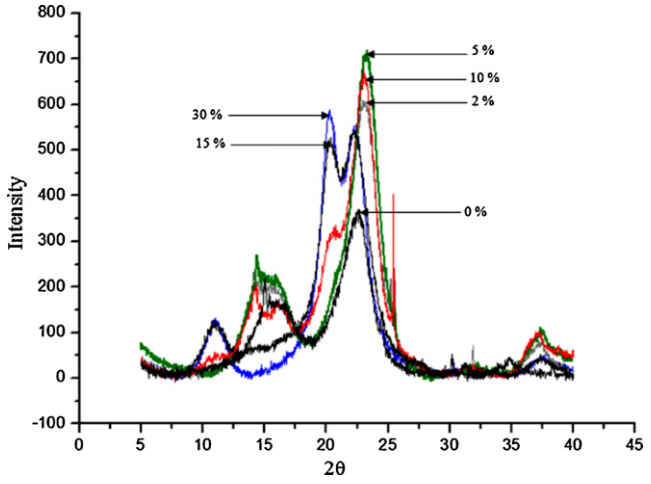

Fig. 1. Corrected X-ray diffractograms of untreated fibres (0% (w/v) NaOH) and alkali treated fibres (2, 5, 10, 15 and 30 w/v NaOH).

All the diffractograms of the treated and untreated samples exhibit considerable overlap of the diffraction peaks. Thus, the peak resolution is the only valid method for obtaining reliable parameters to measure crystallinity and apparent crystallite size. In this study, we exclude crystalline scattering from unidentified phases of noncellulosic origin from the contribution to the total cellulose crystalline scattering.

Fig. 2 represents an example of peak deconvolution for 10% NaOH treated fibres. The profiles are resolved into *n* peaks for each cellulose polymorph (cellulose I and II) and the calculated intensities are obtained by summing these *n* peaks. The number of peaks (*n*) depends on the fibre treatment.

Fig. 3 shows the percentages (in area) of CI and CII peaks versus NaOH concentration. It can be observed, for low alkali concentrations, that the major crystalline peak occurs at 2θ = 23°, which represents the crystallographic plane (0 0 2) of cellulose I. When transformed to cellulose II, the major peaks are located at 2θ = 20° and 2θ = 22°, which represent the crystallographic planes (1 0 $\bar{1}$) and (0 0 2) of cellulose II, respectively.

For the extremely low NaOH concentrations (<1% w/v), only the 4 peaks characteristic of cellulose I are present. These peaks are approximately located at 2θ = 15°, 16°, 20° and 22°; which are the positions of the (1 0 1), (1 0 $\bar{1}$), (0 2 1) and (0 0 2) crystallographic plane reflections, respectively. When treated with 2% (w/v) NaOH, the polymorphic transformation of cellulose I to cellulose II begun as indicated by the appearance of the diffraction at 2θ = 20° resulting from the (1 0 $\bar{1}$) lattice plane of cellulose II (Zhou et al., 2004). At 5% (w/v) NaOH concentration, an additional peak at 2θ = 22° that corresponds to the (0 0 2) lattice plane of cellulose II appears, thus enhancing the mercerisation process. The mercerisation phenomenon is achieved for the alkali concentration of 15% by the appearance of the 3 peaks characteristic of cellulose II at 2θ = 11°, 20° and 22° (Beatriz et al., 2006; Chen et al., 2008; Ouajai & Shanks, 2005; Raymond et al., 1995; Sang et al., 2005).

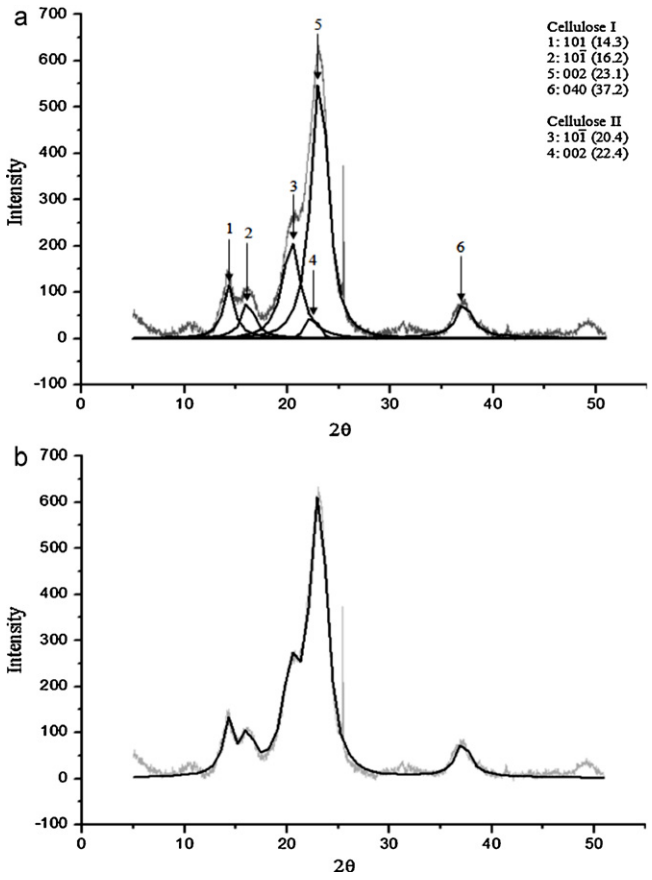

Fig. 2. X-ray diffractogram analysis of alkali treated fibres (10% (w/v) NaOH). (a) Profiles of the resolved peaks and (b) observed and calculated intensities.

3.2. Polymorphic transformation from cellulose I to cellulose II

When treated with caustic soda, fibre goes through four different stages:

- swelling
- dissolution
- mercerisation
- and degradation.

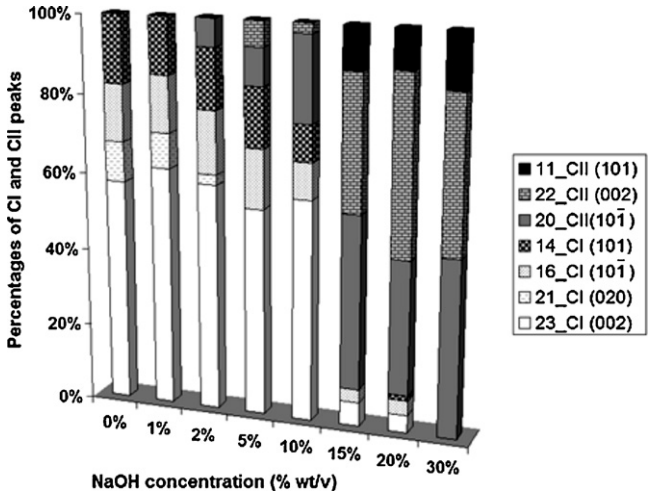

Fig. 3. Percentages (in area) of CI and CII peaks versus NaOH concentration.

3.2.1. Swelling and dissolution

These phenomena are strongly dependent on treatment temperature and soda concentration.

The dissolution (or in a less extent the swelling) of cellulose is an essential step to make it react. Without a preliminary swelling, only a superficial reaction in the fibre is possible. When the fibre swells, the whole structure of the cellulose is conserved despite the increase in mass due to the soda absorption and the significant changes of the fibre physical properties. On the other hand, the dissolution of cellulose induces the transition from a biphase system to a monophase one, and the initial supramolecular structure of the fibre is destroyed.

Despite these small differences, both swelling and dissolution phenomena have common characteristics. In both cases, intermolecular forces between macromolecules are supplanted by stronger interactions between molecular chains and caustic soda, leading to the destruction of the cellulose supramolecular structure. The swelling and dissolution process increase the hydroxyl groups' accessibility. There is no determinate limit between swelling and dissolution phenomena and caustic soda may cause at the same time swelling or dissolution of cellulose depending on the initial structure.

The cellulose swelling is a complicated process which affects both molecular and supramolecular structures.

At the molecular level, the strong interactions between hydroxyl groups and sodium hydrate lead to the rupture of inter and intramolecular bonds. The solvation spheres of the sodium hydroxide ions play an important role for the cellulose/soda interaction. They act to separate the cellulose chains.

In a first step, water molecules penetrate the amorphous regions of cellulose where hydrogen bonds are destroyed. Then, the sodium hydrate reaches the crystalline zones and reacts with anhydroglucose hydroxyl groups. Gradually, the original stabilisation of cellulosic structure due to the inter and intramolecular hydrogen bonds is replaced by additional binding between hydroxycelllulosic groups and Na^+ and OH^- sodium hydroxide ions.

At the supramolecular level, modifications of crystal size dimensions and chain conformations are detected for the alkali concentration corresponding to maximum swelling. The swelling of the fibre in alkali solution alters the crystalline and amorphous proportions of the alkali cellulose. This modification of native cellulose crystalline structure may be detected by X-ray diffraction. Stable ternary complexes "cellulose/soda/water" called soda celluloses (Na Cell) are formed with different conformations depending on the temperature treatment and the alkali concentration.

3.2.2. Mercerisation

Mercerisation is the alkali treatment of cellulose which induces irreversible transformation of the crystalline structure from native cellulose (cellulose I) to mercerised cellulose (cellulose II), going through different crystalline complexes called soda celluloses (Na Cell) (Kayoko et al., 2011). The crystal packing of chains initially aligned in parallel for native cellulose I is rearranged in anti-parallel chains characteristic of cellulose II. During this transformation, the alkali solution penetrates the amorphous regions located between crystallites. The penetration of the alkali solution in the less ordered regions leads to the formation of soda cellulose I which has a little effect on the chain conformation and the crystalline regions. Nevertheless, the formation of soda cellulose I with anti-parallel chains is favourite and it results in gradual decrease of cellulose I crystalline regions leading to the formation of soda cellulose I crystallites. Following this first step, soda cellulose I becomes able to absorb more alkali solution and then it is converted into soda cellulose II with helical structure. By washing Na Cellulose II, all NaOH is eliminated and the final structure of Na Cell IV is obtained and converted to cellulose II by drying. Table 1 gives the unit cell dimensions (found in

Table 1
Unit cell dimensions of different cellulose allomorphs.

Type	Reference	Number of chains	Unit cell (Å,°)					
			a	*c*	*b*	*α*	*γ*	*β*
I_α	Sugiyama et al. (1991)	1	6.74	5.93	10.36	117	113	81
I_β	Finkenstadt & Millane (1998)	2	7.85	8.27	10.38	90	90	96.3
II mercer.	Langan et al. (2001)	2	8.10	9.05	10.31	90	90	117.1
Na-Cell I	Nishimura & Sarko (1991)	4	8.83	25.28	10.29	90	90	90.0
Na-Cell IV	Keller (1992)	2	9.57	8.72	10.35	90	90	122.0

the literature) of the different cellulose polymorphs that go through mercerisation process (Zugenmaier, 2001).

Based on the previous single crystal and powder diffraction studies (Fink, Hofmann, & Philipp, 1995; Kolpak & Blackwell, 1976; Langan, Nishiyama, & Chanzy, 1999; Langan, Nishiyama, & Chanzy, 2001; Mansikkamäki, Lahtinen, & Rissanen, 2005; Nishiyama et al., 2003; Okano & Koyanagi, 1986; O'Sullivan, 1997; Raymond et al., 1995), two characteristic diffraction peaks ($2\theta = 14.6°$, 16.1°) of polymorph CI and one diffraction peak ($2\theta = 12.1°$) of CII were selected as probes for the conversion from CI to CII in the mercerization conditions. Some analysis methods for monitoring the conversion can already be found in the literature (Ruland, 1961; Rånby, 1952; Sao, Samantaray, & Bhattacherjee, 1994). However, in our case, these methods were not applied as such but were used as a basis for the presented method.

Fig. 4 shows the extent of the conversion from cellulose I to cellulose II during mercerisation process. The major cellulose transformation (corresponding to the mercerisation process) occurs between 10% and 15% NaOH concentration. At NaOH concentrations inferior to 10%, cellulose I is dominating in the fibre and only swelling and dissolution phenomena exist, whereas for NaOH concentrations exceeding 15%, cellulose II is the major component in the fibre and the degradation process occurs at these high concentrations.

Besides, it is worth noting that the conversion from cellulose I to cellulose II is associated with a significant decrease in the percent crystallinity and therefore in the mechanical properties of the fibre (Sotton et al., 1978). As seen in Figs. 5 and 8, the crystallinity index as well as the tenacity values present a drop for 10–15% NaOH concentrations, this is assumed to be due to an overall disorder in the fibre which occurs at the moment of cellulose polymorphic transformation.

3.3. Percent crystallinity

The crystallinity index of the treated and untreated agave samples were calculated using Eq. (7) which is described in Section 2.

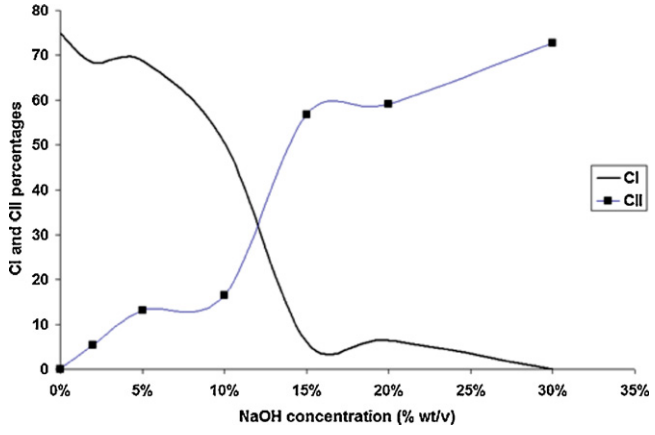

Fig. 4. Conversion from cellulose I to cellulose II during mercerisation process.

The results, shown in Fig. 5, represent the variation of the crystallinity index with the NaOH concentration. It can be seen from Fig. 5 that the crystallinity index of agave fibre increased for alkali treatments not exceeding 2% (w/v). This is thought to be due to better packing and stress relaxation of cellulose chains as a result of the removal of pectins and other amorphous constituents from the fibre. In contrast, higher NaOH concentrations (>2%) induce a considerable decrease of the crystallinity index. At this level, mercerization phenomenon occurs altering the fine structure and morphology of the fibre as well as the conformation of the cellulose chains. During this process, the alkali penetrates the cellulose fibre and the material swells. The polysaccharide chains are rearranged from native cellulose I (chains aligned in parallel) to cellulose II (anti-parallel); the amount of less ordered material in the fibre rises, while the crystalline part contracts. In the same manner, some authors reported about changes in the crystallinity through alkaline treatment on hemp (Mirjana et al., 2008), coir (Sreenivasan, Bahama, & Iyer Krishnan, 1996; Varma, Varma, & Varma, 1984) and flax (Sharma, Fraser, McCall, & Lyons, 1995) fibres. Though the optimum NaOH concentration value (corresponding to the higher crystallinity index) depends on the type of fibre, it remains at the order of 2–5% (w/v) NaOH for the tested fibres.

3.4. Unit cell dimensions and crystallite sizes

The different definitions of the cellulose unit cells in the literature may cause slight uncertainties in the peak designations as reviewed recently by O'Sullivan (1997). The differences are partially due to continually evolving knowledge about the arrangement of the cellulose chains in the unit cell (Gardner & Blackwell, 1974; Honjo & Watanabe, 1958; Langan et al., 1999, 2001; Meyer & Misch, 1937; Sarko & Muggli, 1974; Sugiyama et al., 1991; Wada, Okano, & Sugiyama, 1997; Woodcock & Sarko, 1980). The uncertainties arise from the fact that native cellulose consists of two polymorphs, the more recently found triclinic form designated as I_α and the monoclinic polymorph designated as I_β (Nishiyama et al., 2003; VanderHart & Atalla, 1984). In addition, the choice of the unique axis in the monoclinic crystal systems of cellulose varies in the literature due to historical reasons (Young, 1986). The original choice of the unit cell axes in the monoclinic crystal system was generally performed so that the *b*-axis (fibre axis) was set unique with an acute β angle ($\beta \neq 90°$) following the classical Meyer–Mark–Misch model. Nowadays a unique *c*-axis is generally preferred in the case of cellulose unit cells ($\gamma \neq 90°$). Fink, Hofmann, and Philipp (1995) have presented a comparison of peak designations of two different crystallographic settings of monoclinic unit cells of CI; this was reported earlier by Meyer and Misch (1937) and Sugiyama et al. (1991). Depending on the selection of the monoclinic cell setting, the lattice planes of, for example, diffraction peaks 14.7°, 16.1° and 22.5° (2θ) of polymorph CI can be designated as $(1\ \bar{1}\ 0)$, $(1\,1\,0)$, $(2\,0\,0)$ according to Sugiyama, while in the Meyer–Mark–Misch system the planes have indices of $(1\,0\,1)$, $(1\ 0\ \bar{1})$ and $(0\,0\,2)$, respectively. Finally, it should be pointed out that the 2θ values of the diffraction peaks vary slightly in the previous publications due to several obvious factors such as the quality of instrumentation,

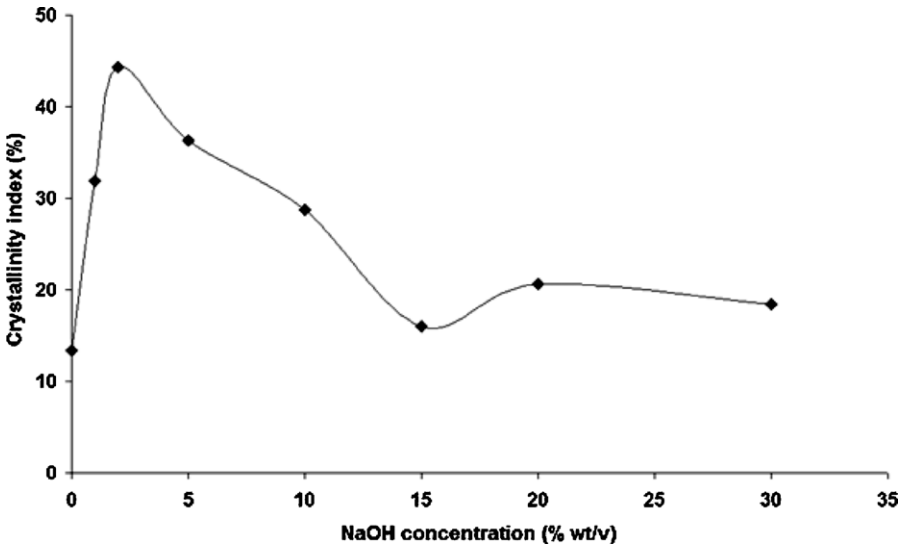

Fig. 5. Crystallinity index versus NaOH concentration.

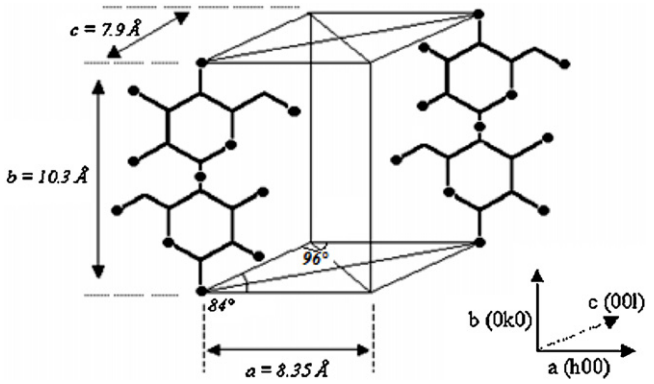

Fig. 6. Unit cell dimensions of cellulose I.

experimental setups, general crystallinity and mixing ratio of the cellulose polymorphs and finally the "biological origin" of the samples analyzed. In this work, we use the Meyer–Mark–Misch system to represent the cellulose unit cell. In this case, native cellulose (cellulose I_β) has a monoclinic unit cell with the dimensions shown in Fig. 6 (Champetier & Monnerie, 1969; Morton & Hearle, 1975).

The cellulose molecule consists of a series of glucose rings linked together by valency bonds and situated in the *ab* plane (Fig. 6). Cellulosic chains are arranged parallel to the *b* axis which represents fibre axis. Hydroxyl groups of these macromolecular chains are joined laterally by means of hydrogen bonds (Champetier & Monnerie, 1969; Morton & Hearle, 1975).

Table 2 exhibits results for the unit cell dimensions (a, b, c and β) of the tested samples. It is clear from this table that crystallographic parameters are greatly affected by the fibre treatment. The unit cell parameters of untreated fibres closely match the values reported in the literature for native cellulose (Champetier & Monnerie, 1969; Morton & Hearle, 1975). By treating fibres with different alkali concentrations, the unit cell dimensions are modified.

As described in the previous section (Section 3.2), the path from cellulose I to cellulose II goes by way of Na-celluloses. It results from the formation of different alkali celluloses during the mercerisation process that the unit cell parameters of *A. americana* L. fibre, as seen in Table 2, vary with the NaOH concentration. Particularly, the monoclinic angle values (β) correlate with those found in the literature.

From Table 2, it is also clear that the length of repeating unit in cellulose (b) have not been altered with the alkali treatment. It remains at the order of 10.3 Å.

The variation of the microcrystallite sizes $D_{\perp hkl}$ of (1 0 1), (1 0 $\bar{1}$) and (0 0 2) crystallographic planes is shown in Fig. 7. The crystallite size is decreased to a constant value for fibres treated at higher than 15% (w/v) NaOH. This may be due to the penetration of alkali solution in the crystalline regions to form soda celluloses, resulting in an overall disorder in the fibre crystallites. This disorder is evidenced by a decrease in both crystallite size and crystallinity index.

3.5. Mechanical properties

From the results in Fig. 8, it can be seen that the alkali treatment concentration has an effect on the tensile strength of the

Table 2
Unit cell dimensions a, b, c and β of the untreated and alkali treated samples of *Agave americana* L. fibres.

NaOH concentration (%)	CI				CII			
	a (Å)	b (Å)	c (Å)	β (°)	a (Å)	b (Å)	c (Å)	β (°)
0	6.1	10.73	8.48	106	–	–	–	–
1	7.49	10.32	9.25	120	–	–	–	–
2	7.38	10.32	9.05	118	–	–	–	–
5	7.33	10.27	8.84	116	–	–	–	–
10	7.41	10.32	9.09	119	7.41	10.32	9.09	119
15	–	–	–	–	7.2	10.27	8.96	114
20	7.13	10.32	8.7	120	7.2	10.32	8.96	114
30	–	–	–	–	6.1	10.32	8.86	114

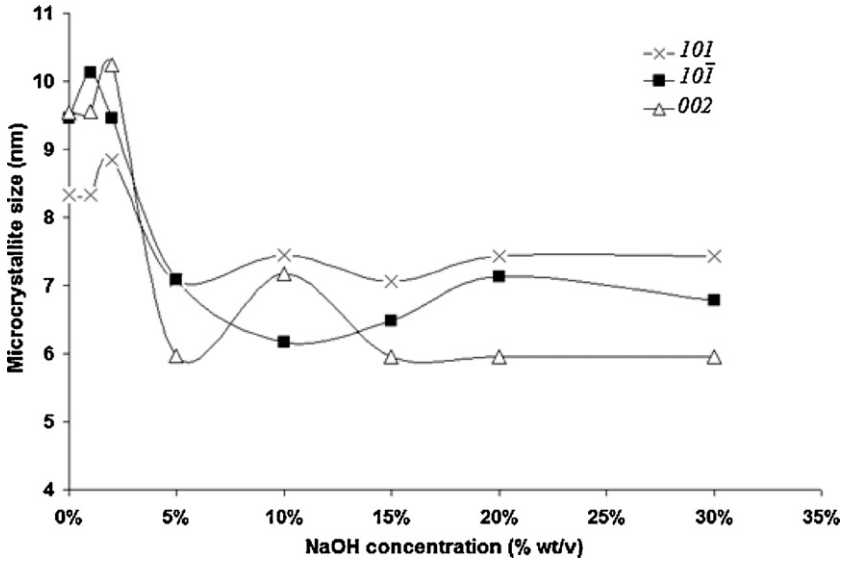

Fig. 7. Variation of the microcrystallite sizes $D_{\perp h\,k\,l}$ of (1 0 1), (1 0 $\bar{1}$) and (0 0 2) crystallographic planes with NaOH concentration.

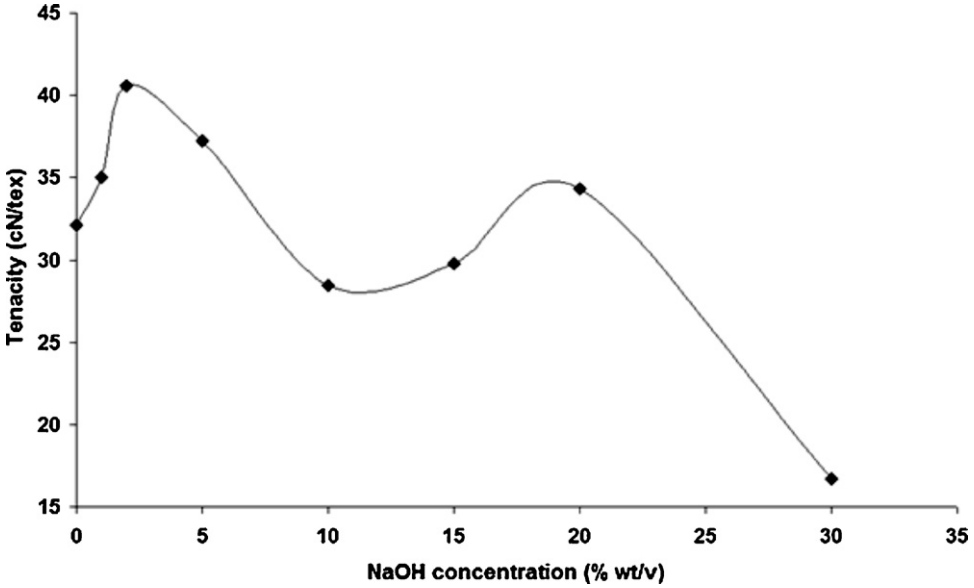

Fig. 8. Variation of the tenacity with the NaOH concentration.

treated fibres (Aboul-Fadl, Zeronian, Kamal, Kim, & Elisson, 1985). Treatments with low alkali concentrations produce fibres that are stronger than the untreated fibres, whereas treatments with high concentrations (>2% w/v) result in weaker fibres.

Actually, for low concentration treatments, the hemicelluloses are removed and the interfibrillar region is likely to be less dense and less rigid and thereby makes the fibrils more capable of rearranging themselves along the direction of tensile deformation. When natural fibres are stretched, such rearrangements amongst the fibrils would result in better load sharing by them and hence result in higher stress development in the fibre.

The tenacity increase is also related to the increase of crystallinity index found in the previous section (Section 3.3). In contrast, the decrease in strength for higher alkali concentrations (>2% w/v) can be attributed to the degradation of cellulose at these concentrations and to the transition from cellulose I to cellulose II as cellulose II generally displays a lower chain modulus. Actually, the modulus of the cellulose I chain is around 140 GPa, while that of cellulose II is 90 GPa (Northolt et al., 2001). These have important consequences for the ultimate tensile properties of the alkali treated fibres which generally would imply inferior tenacity values compared with untreated fibres.

The crystalline character of *A. americana* L. fibres reveals their mechanical properties. As seen in the curves of Figs. 5 and 8 which have exactly the same shape, the crystallinity index is an important factor which directly influences the tenacity of the fibre. In other words, the higher the degree of crystallinity is, the stronger and more rigid the fibres are and vice versa.

4. Conclusions

The work we have presented in this paper reports on the effect of alkali treatment on the mercerisation process of *A. americana* L. fibres and the transition from cellulose I to cellulose II polymorphs. The crystalline structure of the cellulose treated with different NaOH concentrations was analyzed by wide-angle

X-ray diffraction. From this study, it was found that the major cellulose transformation (corresponding to the mercerisation process) occurs between 10% and 15% NaOH concentrations. For lower NaOH concentrations, cellulose I is dominating in the fibre and only swelling and dissolution phenomena exist. A treatment with 2% alkali concentration produces the strongest fibres due to the removing of noncellulosic components and at this level, no polymorphic transformation is still detected. For high NaOH concentrations (exceeding 15%), fibre degradation occurs and it results in a significant decrease on the mechanical properties. During the mercerisation process, it results from the formation of different alkali celluloses that the unit cell parameters as well as the crystallite sizes of *A. americana* L. fibre vary significantly with the NaOH concentration.

From this study, it can also be deduced that the crystallinity index strongly depends on the alkali concentration. It reaches the highest value for 2% (w/v) NaOH and this is thought to be due to better packing of the cellulose chains with the removal of amorphous materials from the fibre. On the other hand, the crystallinity index undergoes an accidental drop for 10–15% NaOH concentrations associated with the conversion from cellulose I to cellulose II. This is assumed to be due to an overall disorder in the fibre which occurs at the moment of cellulose polymorphic transformation.

References

Aboul-Fadl, A. M., Zeronian, S. H., Kamal, M. M., Kim, M. S., & Elisson, M. S. (1985). Effect of mercerization on the relation between single fiber mechanical properties and fine structure for different cotton species. *Textile Research Institute*, *55*, 461–469.

Akerholm, M., Hinterstoisser, B., & Salmen, L. (2004). Characterization of the crystalline structure of cellulose using static and dynamic FT-IR spectroscopy. *Carbohydrate Research*, *339*, 569–578.

Atalla, R. H., & VanderHart, D. L. (1999). The role of solid state ^{13}C NMR spectroscopy in studies of the nature of native celluloses. *Solid State Nuclear Magnetic Resonance*, *15*, 1–19.

Beatriz, A. P., Assa, M. N., & Belgacemb, E. F. (2006). Mercerized linters cellulose: Characterization and acetylation in N,N-dimethylacetamide/lithium chloride. *Carbohydrate Polymers*, *63*, 19–29.

Beg, M. D. H., & Pickering, K. L. (2004). Effect of fibre pre-treatment on the mechanical properties of wood/polypropylene composites. In *Proceedings of the 2nd International Conference on Structure, Processing and Properties of Materials, February, Dhaka, Bangladesh* (pp. 240–247).

Berlant, A., & Khalifa. (1991). Crystalline character of native and chemically treated Saudi Arabian cotton fibers. *Textile Research Journal*, *61*(10), 602–608.

Bledzki, A. K., Fink, H. P., & Specht, K. (2004). Unidirectional hemp and flax EP and PP-composites: Influence of defined fiber treatments. *Journal of Applied Polymer Science*, *93*, 2150–2156.

Cael, J. J., Gardner, K. H., Koenig, J. L., & Blackwell, J. J. (1975). Infrared and Raman spectroscopy of carbohydrates. Normal coordinate analysis of cellulose I. *Journal of Chemical Physics*, *62*, 1145–1153.

Chaâbouni, Y. (2005). Cractérisation de la microstructure de la fibre d'*Agave americana* L. Contribution à l'étude de composites renforcés par des fibres d'agave, PhD Thesis, Université de Haute Alsace, Mulhouse, France.

Champetier, G., & Monnerie, L. (1969). *Introduction à la chimie macromoléculaire*. Paris: Masson et CIE.

Chen, Q., Nattakan, S., Ni, X., & Ton, P. (2008). The effect of fibre volume fraction and mercerization on the properties of all-cellulose composites. *Carbohydrate Polymers*, *71*, 458–467.

Colom, X., & Carrillo, F. (2002). Crystallinity changes in lyocell and viscose-type fibres by caustic treatment. *European Polymer Journal*, *38*, 2225–2230.

Davidson, T. C., Newman, R. H., & Ryan, M. J. (2004). Variations in the fiber repeat between samples of cellulose I from different sources. *Carbohydrate Research*, *339*, 2889–2893.

Dinand, E., Vignon, M., Chanzy, H., & Heux, L. (2002). Mercerization of primary wall cellulose and its implication for the conversion of cellulose I → cellulose II. *Cellulose*, *9*, 7–18.

El Oudiani, A., Chaâbouni, Y., Msahli, S., & Sakli, F. (2009). Physico-chemical characterisation and tensile mechanical properties of *Agave americana* L. fibres. *The Journal of The Textile Institute*, *100*(5), 430–439.

Fink, H. P., Hofmann, D., & Philipp, B. (1995). Some aspects of lateral chain order in cellulosics from X-ray scattering. *Cellulose*, *2*, 51–70.

Finkenstadt, V. L., & Millane, R. P. (1998). Crystal structure of *Valonia* cellulose Iβ. *Macromolecules*, *31*, 3776–3778.

Forman, D. W., & Jakes, K. A. (1993). X-ray diffractometric measurement of microcrystallite size, unit cell dimensions, and crystallinity: Application to cellulosic marine textiles. *Textile Research Journal*, 455–464.

Gardner, K. H., & Blackwell, J. (1974). The structure of native cellulose. *Biopolymers*, *13*, 1975–2001.

Gassan, J., & Bledzki, A. K. (1999a). Alkali treatment of jute fibers: Relationship between structure and mechanical properties. *Journal of Applied Polymer Science*, *71*, 623–629.

Gassan, J., & Bledzki, A. K. (1999b). Possibilities for improving the mechanical properties of jute/epoxy composites by alkali treatment of fibres. *Composites Science and Technology*, *59*(9), 1303–1309.

Gert, E. V., Socarras-Morales, A., Zubets, O. V., Shishonok, M. V., Torgashov, V. I., Matyulko, A. V., et al. (2001). New methods for the preparation of cellulose II powder forms of various morphology. *Cellulose Chemistry and Technology*, *35*, 417–427.

Gumuskaya, E., Usta, M., & Kirci, H. (2003). The effects of various pulping conditions on crystalline structure of cellulose in cotton linters. *Polymer Degradation Stability*, *81*, 559–564.

Honjo, G., & Watanabe, M. (1958). Examination of cellulose fiber by the low-temperature specimen method of electron diffraction and electron microscopy. *Nature*, *181*, 326–328.

Jähn, A., Schröder, M. W., Füting, M., Schenzel, K., & Diepenbrock, W. (2002). Characterization of alkali treated flax fibres by menas of FT Raman spectroscopy and environmental scanning electron microscopy. *Spectrochimica Acta*, *58*, 2271–2279.

Kayoko, K., Satoshi, K., Eiji, T., & Masahisa, W. (2011). Crystal transition from Na-cellulose IV to cellulose II monitored using synchrotron X-ray diffraction. *Carbohydrate Polymers*, *83*, 483–488.

Keller, E. (1992). SCHAKAL 92: A computer program for graphic representation of molecules and crystallographic models. D-79104 Freiburg i. Br.

Klemm, D., Philipp, B., Heinze, T., Heinze, U., & Wagenknecht, W. (1998). *Comprehensive cellulose chemistry* Weinheim: Wiley–VCH., pp. 9–25.

Kolpak, F. J., & Blackwell, J. (1976). Determination of the structure of cellulose II. *Macromolecules*, *9*, 273–278.

Kreze, T., & Malej, S. (2003). Structural characteristics of new and conventional regenerated cellulosic fibers. *Textile Research Journal*, *73*(8), 675–684.

Kroschwitz, J. I. (1990). *Polymers: Fibers and textiles: A compendium*. New York: Wiley Pub. Book ISBN: 0471522112.

Langan, P., Nishiyama, Y., & Chanzy, H. (1999). A revised structure and hydrogen-bonding system in cellulose II from a neutron fiber diffraction analysis. *Journal of the American Chemical Society*, *121*, 9940–9946.

Langan, P., Nishiyama, Y., & Chanzy, H. (2001). X-ray structure of mercerized cellulose II at 1 Å resolution. *Biomacromolecules*, *2*(2), 410–416.

Mansikkama¨ki, P., Lahtinen, M., & Rissanen, K. (2005). Structural changes of cellulose crystallites induced by mercerization in different solvent systems; determined by powder X-ray diffraction method. *Cellulose*, *12*, 233–242.

Meyer, K. H., & Misch, L. (1937). Positions des atomes dans le nouveau modele spatial de la cellulose. *Helvetica Chimica Acta*, *20*, 232–244.

Mirjana, K., Biljana, P., & Petar, S. (2008). Quality of chemically modified hemp fibers. *Bioresource Technology*, *99*, 94–99.

Morton, W. E., & Hearle, J. W. S. (1975). *Physical properties of textile fibers* (2nd ed.). London: The Textile Institute/Heinemann.

Msahli, S. (2002), Etude du potentiel textile des fibres d'*Agave americana* L., PhD Thesis, No.°02Mulh0691, Université de Haute Alsace, Mulhouse, France.

Murdock, C. C. (1930). The form of the X-ray diffraction bands for regular crystals of colloidal size. *Physical Review*, *35*, 8–23.

Mwaikambo, L. Y., & Ansell, A. P. (2003). Hemp fibre reinforced cashew nut shell liquid composites. *Composite Science and Technology*, *6*, 1297–1305.

Newman, R. H., & Davidson, T. C. (2004). Molecular conformations at the cellulose–water interface. *Cellulose*, *11*, 23–32.

Nishimura, H., & Sarko, A. (1991). Mercerisation of cellulose. 6. Crystal and molecular structure of Na-cellulose IV. *Macromolecules*, *24*, 771–778.

Nishiyama, Y., Langan, P., & Chanzy, H. J. (2002). Crystal structure and hydrogen-bonding system in cellulose 1 β from synchrotron X-ray and neutron fiber diffraction. *Journal of the American Chemical Society*, *124*, 9074–9082.

Nishiyama, Y., Sugiyama, J., Chanzy, H., & Langan, P. (2003). Crystal structure and hydrogen bonding system in cellulose Ia from synchrotron X-ray and neutron fiber diffraction. *Journal of the American Chemical Society*, *125*, 14300–14306.

Northolt, M. G., Boerstoel, H., Maatman, H., Huisman, R., Veurink, J., & Elzerman, H. (2001). The structure and properties of cellulose fibres spun from an anisotropy phosphoric acid solution. *Polymer*, *42*, 8249–8264.

Okano, T., & Koyanagi, A. (1986). Structural variation of native cellulose related to its source. *Biopolymers*, *25*, 851–861.

O'Sullivan, A. C. (1997). Cellulose: The structure slowly unravels. *Cellulose*, *4*, 173–207.

Ouajai, S., & Shanks, R. A. (2005). Composition, structure and thermal degradation of hemp cellulose after chemical treatments. *Polymer Degradation and Stability*, 327–335.

Perel, J. (1990). An X-ray study of regain-dependent deformations in cotton crystallites. *The Journal of The Textile Institute*, *81*, 241–244.

Prasad, B. M., & Sain, M. M. (2003). Mechanical properties of thermally treated hemp fibers in inert atmosphere for potential composite reinforcement. *Material Research and Innovation*, *7*(231), 231–238.

Proniewicz, L. M., Paluszkiewicz, C., Weselucha-Birczyn˝ska, A., Majcherczyk, H., Baran˝ski, A., & Konieczna, A. (2001). FT-IR and FT-Raman study of hydrothermally degradated cellulose. *Journal of Molecular Structure*, *596*, 163–169.

Rånby, B. G. (1952). The mercerization of cellulose. *Acta Chemica Scandinavica*, *6*, 116–127.

Raymond, S., Kvick, A., & Chanzy, H. (1995). The structure of cellulose II: A revisit. *Macromolecules*, *28*, 8422–8425.
Roncero, M. B., et al. (2005). The effect of xylanase on lignocellulosic components during the bleaching of wood pulps. *Bioresource Technology*, *96*(1), 21–30.
Ruan, D., Zhang, L., Mao, Y., Zeng, M., & Li, X. (2004). Microporous membranes prepared from cellulose in NaOH/thiourea aqueous solution. *Journal of Membrane Science*, *241*, 265–274.
Ruland, W. (1961). X-ray determination of crystallinity and diffuse disorder scattering. *Acta Crystallographica*, *14*, 1180–1185.
Sang, et al. (2005). Crystalline structure analysis of cellulose treated with sodium hydroxide and carbon dioxide by means of X-ray diffraction and FTIR spectroscopy. *Carbohydrate Research*, *340*, 2376–2391.
Sao, K. P., Samantaray, B. K., & Bhattacherjee, S. (1994). X-ray study of crystallinity and disorder in ramie fiber. *Journal of Applied Polymer Science*, *52*, 1687–1694.
Sarko, A., & Muggli, R. (1974). Packing analysis of carbohydrates and polysaccharides. III. Valonia cellulose and cellulose II. *Macromolecules*, *7*, 486–494.
Scherrer, P. (1918). Bestimmung der Grosse und inneren Struktur von Kolloidteilchen mittels Rontgenstrahlen. *Nachrichten Gesellschaft der Wissenschaften zu Göttingen*, *2*, 8–100.
Schwanninger, M., Rodrigues, J. C., Pereira, H., & Hinterstoisser, B. (2004). Effects of short-time vibratory ball milling on the shape of FTIR spectra of wood and cellulose. *Vibrational Spectroscopy*, *36*, 23–40.
Sharma, H. S. S., Fraser, T. W., McCall, D., & Lyons, G. (1995). Fine structure of chemically modified flax fiber. *The Journal of the Textile Institute*, *86*, 539–548.
Sotton, M., Arniaud, A. M., & Rabourdin, C. (1978). Etude par diffractomérie des rayons X des paramètres de cristallinité et de désordre dans les fibres textiles. *Bulletin Scientifique ITF*, *7*(27), 265–290.
Sreenivasan, S., Bahama, I. P., & Iyer Krishnan, K. R. (1996). Influence of delignification and alkali treatment on the fine structure of coir fibres (*Cocos nucifera*). *Journal of Materials Science*, *31*(3), 721–726.
Sugiyama, J., Vuong, R., & Chanzy, H. (1991). Electron diffraction study on the two crystalline phases occurring in native cellulose from an algal cell wall. *Macromolecules*, *24*, 4168–4175.
Tserki, V., et al. (2005). A study of the effect of acetylation and propionylation surface treatments on natural fibres. *Composites Part A: Applied Science Manufacturing*, *36*(8), 1110–1118.
VanderHart, D. L., & Atalla, R. H. (1984). Studies of microstructure in native celluloses using solid state ^{13}C NMR. *Macromolecules*, *17*, 1465–1472.
Varma, D. S., Varma, M., & Varma, I. K. (1984). Coir fibers: Part I: Effect of physical and chemical treatments on properties. *Textile Research Journal*, *54*, 827–832.
Wada, M., Okano, T., & Sugiyama, J. (1997). Synchrotron-radiated X-ray and neutron diffraction study of native cellulose. *Cellulose*, *4*, 221–232.
Woodcock, C., & Sarko, A. (1980). Packing analysis of carbohydrates and polysaccharides. II. Molecular and crystal structure of native ramie cellulose. *Macromolecules*, *13*, 1183–1187.
Young, R. A. (1986). Cellulose, structure, modification and hydrolysis. In R. A. Young, & R. M. Rowell (Eds.), *Cellulose* (pp. 3–49). New York: Wiley-Interscience.
Zhou, L. M., Yeung, K. W., Yuen, C. W. M., & Zhou, X. (2004). Characterization of ramie yarn treated with sodium hydroxide and crosslinked by 1,2,3,4-butanetetracarboxylic acid. *Journal of Applied Polymer Science*, *91*, 1857–1864.
Zugenmaier, P. (2001). Conformation and packing of various crystalline cellulose fibers. *Progress Polymer Science*, *26*, 1341–1417.